The EMBO Journal (2012) 31, 1014–1027 | © 2012 European Molecular Biology Organization | All Rights Reserved 0261-4189/12
www.embojournal.org

THE EMBO JOURNAL

Sec24p and Sec16p cooperate to regulate the GTP cycle of the COPII coat

Leslie F Kung[1,5], Silvere Pagant[1,5], Eugene Futai[2], Jennifer G D'Arcangelo[1], Roy Buchanan[1], John C Dittmar[1], Robert JD Reid[3], Rodney Rothstein[3], Susan Hamamoto[2], Erik L Snapp[4], Randy Schekman[2] and Elizabeth A Miller[1,*]

[1]Department of Biological Sciences, Columbia University, New York, NY, USA, [2]Department of Molecular and Cell Biology, University of California, Berkeley, CA, USA, [3]Department of Genetics and Development, Columbia University Medical Center, New York, NY, USA and [4]Department of Anatomy and Structural Biology, Albert Einstein College of Medicine, New York, NY, USA

Vesicle budding from the endoplasmic reticulum (ER) employs a cycle of GTP binding and hydrolysis to regulate assembly of the COPII coat. We have identified a novel mutation (*sec24-m11*) in the cargo-binding subunit, Sec24p, that specifically impacts the GTP-dependent generation of vesicles *in vitro*. Using a high-throughput approach, we defined genetic interactions between *sec24-m11* and a variety of trafficking components of the early secretory pathway, including the candidate COPII regulators, Sed4p and Sec16p. We defined a fragment of Sec16p that markedly inhibits the Sec23p- and Sec31p-stimulated GTPase activity of Sar1p, and demonstrated that the Sec24p-m11 mutation diminished this inhibitory activity, likely by perturbing the interaction of Sec24p with Sec16p. The consequence of the heightened GTPase activity when Sec24p-m11 is present is the generation of smaller vesicles, leading to accumulation of ER membranes and more stable ER exit sites. We propose that association of Sec24p with Sec16p creates a novel regulatory complex that retards the GTPase activity of the COPII coat to prevent premature vesicle scission, pointing to a fundamental role for GTP hydrolysis in vesicle release rather than in coat assembly/disassembly.

The EMBO Journal (2012) **31,** 1014–1027. doi:10.1038/emboj.2011.444; Published online 9 December 2011
Subject Categories: membranes & transport
Keywords: COPII coat; intracellular traffic; vesicle formation

Introduction

Protein traffic within the endomembrane system of eukaryotic cells occurs via transport vesicles that ferry various molecules between compartments. Vesicles are created by cytoplasmic coat proteins that perform two fundamental roles: selection of cargo molecules (and exclusion of residents) and transformation of the donor membrane into highly curved spherical structures (Kirchhausen, 2000; Stagg *et al*, 2007). Coat assembly is often driven by GTP, with a small monomeric GTPase acting as a regulator of coat assembly; in the GTP-bound state, the G-protein recruits additional cargo adaptor proteins and membrane scaffold proteins, which are subsequently released upon GTP hydrolysis. In this way, coat assembly, triggered by GTP binding, couples cargo recruitment with membrane deformation, then GTP hydrolysis permits uncoating to expose the fusion apparatus required for vesicle delivery to the target compartment (Bonifacino and Glick, 2004; Miller and Barlowe, 2010).

Endoplasmic reticulum (ER)-derived transport vesicles are generated by the COPII coat, comprising five proteins that assemble on the cytoplasmic surface of the ER membrane (Barlowe *et al*, 1994). The GTPase, Sar1p, initiates assembly, recruiting the cargo adaptor platform, Sec23p/Sec24p, and the outer coat, Sec13p/Sec31p. In minimally reconstituted systems, these components assemble in a hierarchical manner, with each layer dependent on the previous one (Matsuoka *et al*, 1998; Antonny *et al*, 2001). Furthermore, each layer of the COPII coat contributes to the GTP cycle by stimulating the relatively poor GTPase activity of Sar1p. Sec23p is the GTPase-activating protein (GAP) for Sar1p (Yoshihisa *et al*, 1993), contributing catalytic residues to the hydrolysis reaction (Bi *et al*, 2002). Sec31p potentiates the action of Sec23p by optimally positioning the catalytic pocket (Antonny *et al*, 2001; Bi *et al*, 2007). Therefore, maximal GTPase activity is achieved only upon full coat assembly. On synthetic liposomes, coat assembly in the presence of GTP is remarkably transient since both the Sec23/24p and Sec13/31p layers have low affinity for Sar1p●GDP (Antonny *et al*, 2001). Thus, intrinsic GTPase regulation by coat proteins themselves creates a paradox: how is coat assembly stabilized for a sufficient amount of time to generate a vesicle when the fully assembled coat triggers its own disassembly? The existence of additional factors required *in vivo* for the negative regulation of Sar1p GTPase activity and/or stabilization of the COPII coat after GTP hydrolysis by Sar1p has long been postulated.

Several lines of evidence point to Sec16p as a potential regulator of COPII vesicle biogenesis. Sec16p is essential for ER-to-Golgi transport *in vivo* (Kaiser and Schekman, 1990), is predominantly localized at ER exit sites and is important for their organization in *Pichia pastoris*, mammals and *Drosophila* (Watson *et al*, 2006; Bhattacharyya and Glick, 2007; Iinuma *et al*, 2007; Ivan *et al*, 2008; Hughes *et al*, 2009). Purified Sec16p is not strictly required for COPII vesicle formation from synthetic liposomes, but clearly stimulates this process (Matsuoka *et al*, 1998; Supek *et al*, 2002). Sec16p is large (~240 kDa), forms oligomers and interacts with all COPII coat proteins (Espenshade *et al*, 1995; Gimeno *et al*, 1996; Shaywitz *et al*, 1997; Whittle and Schwartz, 2010). Taken together, these data suggest that Sec16p acts as a

*Corresponding author. Department of Biological Sciences, Columbia University, 1212 Amsterdam Ave MC2456, New York, NY 10027, USA. Tel.: +1 212 854 2264; Fax: +1 212 865 8246;
E-mail: em2282@columbia.edu
[5]These authors contributed equally to this work

Received: 10 June 2011; accepted: 15 November 2011; published online: 9 December 2011

platform for COPII protein assembly that would nucleate oligomerization or organization of dispersed COPII subunits. The model that the stabilizing role of Sec16p on COPII assembly is structural rather than catalytic is sustained by the observation that purified Sec16p had no effect on Sar1p GTPase activity *in vitro* (Supek *et al*, 2002).

In addition to functioning in simple binding and release of the COPII coat, the GTPase activity of Sar1p also appears to play a role in vesicle scission and cargo recruitment. Either deleting the N-terminal amphipathic α-helix of Sar1p or abrogating Sar1p GTPase activity causes defects in vesicle release, with spherical buds remaining attached to the donor membrane (Bielli *et al*, 2005; Lee *et al*, 2005). These observations suggest that the membrane curvature induced by the N-terminal helix (Lee *et al*, 2005), oligomerization of Sar1p (Long *et al*, 2010) and the lipid destabilization (Settles *et al*, 2010) that accompanies helix insertion and removal during the GTPase cycle are important for scission of the vesicle neck. The potential involvement of GTPase activity in cargo capture was suggested by single molecule fluorescence studies that showed improper clustering of the cargo protein, Bet1p, in the presence of a non-hydrolysable GTP analogue (Tabata *et al*, 2009). However, the mechanism by which GTP hydrolysis might impact the process of cargo capture in the context of a complex membrane remains unclear, in particular, in light of numerous experiments that have delineated Sec24p as the cargo-binding component of the COPII coat (Miller *et al*, 2002, 2003; Mossessova *et al*, 2003; Mancias and Goldberg, 2008).

A combination of genetic, biochemical and structural analyses have clearly defined the cargo-binding function of Sec24p (Miller *et al*, 2003; Mossessova *et al*, 2003). In contrast, Sec24p had no influence on the GTP cycle of Sar1p when tested in a minimal system using only the purified COPII coat proteins (i.e., Sar1p, Sec23/24p and Sec13/31p; Bi *et al*, 2007), suggesting a function as a relatively inert platform that co-opts cargo via direct interaction with ER export signals on its various clients. In this study, we demonstrate that a fragment of Sec16p functions to negatively regulate the Sec23p- and Sec31p-stimulated GTPase cycle of Sar1p. We show that this activity is surprisingly dependent on Sec24p. Finally, we report that the effect of altering this regulation, via a new mutation in Sec24p, results primarily in the release of small COPII vesicles, suggesting a novel role for both Sec24p and Sec16p in regulating the GTP cycle of the COPII coat to prevent premature vesicle release.

Results

Three independent cargo-binding sites have been well defined on yeast Sec24p (Miller *et al*, 2003; Mossessova *et al*, 2003), and the identification of additional cargo-binding sites on mammalian isoforms of Sec24p (Farhan *et al*, 2007; Mancias and Goldberg, 2008) coupled with the observation that many yeast cargo proteins remain unaffected by mutation in the three yeast sites (Miller *et al*, 2003, 2005) raises the prospect that additional sites of cargo interaction remain to be identified. In searching for such sites, we employed an alanine-scanning mutagenesis approach to isolate novel surface mutations on Sec24p. One such mutant, termed *sec24-m11*, contained alterations in two adjacent acidic residues (E504 and D505) on a surface loop flanking the so-called

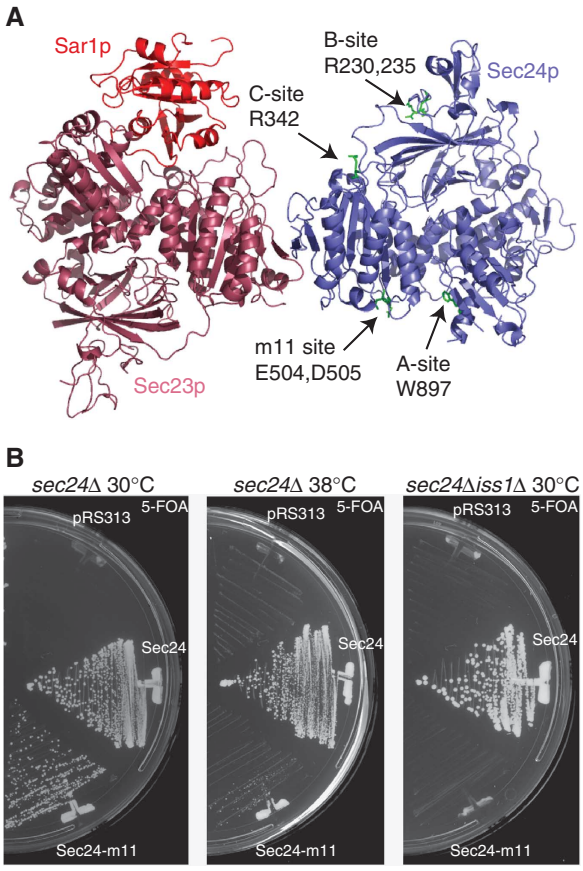

Figure 1 The m11 site defines a novel mutation on the surface of Sec24p. (**A**) The structure of Sar1p, Sec23p and Sec24p showing the positions of the known cargo-binding sites, the A-, B- and C-sites. A novel mutation, the m11 site, is located on a surface loop adjacent to the A-site. (**B**) The phenotype associated with the m11 mutation of Sec24p was assessed by introducing the mutant gene into strains containing chromosomal deletions in *SEC24* and *ISS1* as indicated and testing the ability of these strains to grow in the presence of 5-FOA, which counterselects for a plasmid-borne copy of *SEC24*. In a *sec24*Δ strain, *sec24-m11* was able to confer viability at 30°C (left panel) but growth was significantly impaired at 38°C (middle panel), and in the context of a *sec24*Δ *iss1*Δ double null strain was unable to support viability (right panel).

'A-site' or Sed5p-binding site (Figure 1A). This double mutant was temperature sensitive when present as the sole copy of Sec24p and was unable to support viability at any temperature in a *sec24*Δ *iss1*Δ double-mutant background, where the close Sec24p paralogue, Iss1p, was also deleted (Figure 1B). We tested the phenotypes of the single mutations, E504A or D505A, and detected no growth defects in either a *sec24*Δ or a *sec24*Δ *iss1*Δ background (EAM, unpublished observations), suggesting that preserving a single acidic residue suffices for viability.

The m11 mutation in Sec24 impedes secretion in vivo and causes ER membrane accumulation

We examined secretory pathway function in cells where the sole copy of Sec24p contained the E504A and D505A mutations. Both the GPI-anchored cell wall protein, Gas1p, and the soluble vacuolar hydrolase, CPY, were profoundly delayed in their maturation from precursor ER forms to Golgi-modified forms, suggesting a block in ER exit at restrictive temperature

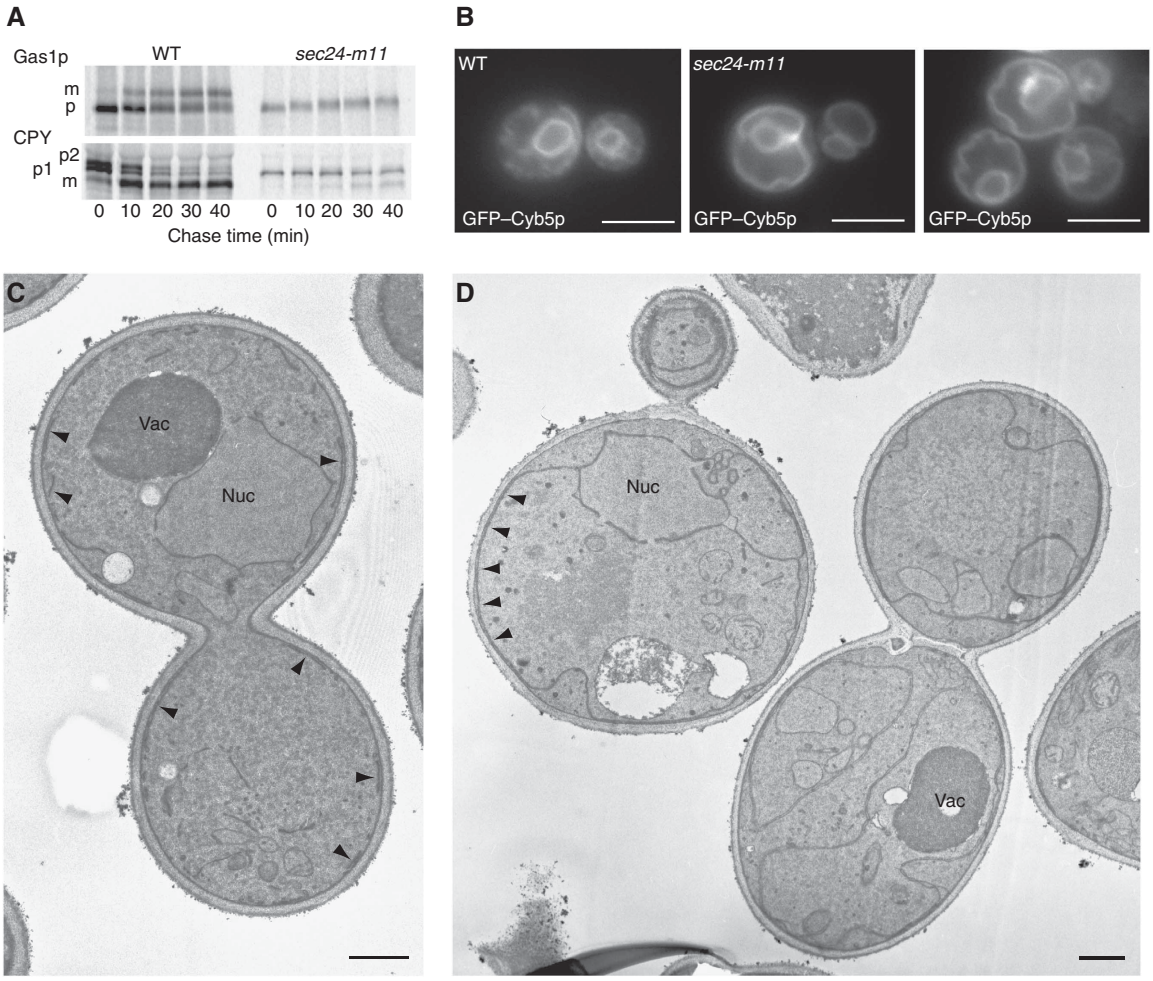

Figure 2 Sec24p-m11 blocks secretion and causes accumulation of ER membranes. (**A**) Maturation of Gas1p or CPY was monitored by pulse-chase analysis after shift to 37°C. Gas1 underwent rapid conversion from the ER precursor (p) form to the Golgi-modified mature (m) form in wild-type cells, whereas this maturation was largely absent from cells expressing Sec24p-m11 as the sole copy of Sec24p. Similarly, CPY accumulated as its ER p1 form in Sec24p-m11 cells but matured normally to Golgi-modified p2 and vacuolar mature (m) forms in wild-type cells. (**B**) Live-cell images of wild-type (left panel) or *sec24-m11* (centre and right panels) strains expressing the ER marker protein, GFP–Cyb5p, following shift to 37°C for 1 h prior to imaging. The *sec24-m11* mutant strain exhibits proliferated internal membranes adjacent to the plasma membrane, consistent with accumulation of cortical ER. Scale bar is 5 μm. (**C**) TEM images of wild-type cells grown at 37°C reveal the endoplasmic reticulum surrounding the nucleus (Nuc) with small strands of cortical membrane underlying the plasma membrane (arrowheads). The vacuole (Vac) stains darkly. Scale bar is 500 nm. (**D**) TEM analysis of *sec24-m11* cells shifted to 37°C for 1 h prior to fixation shows elaborated strands of membrane extending from the nucleus that completely fill the cortical areas of the cell adjacent to the plasma membrane (arrowheads), as well as large internal accumulations of membranes, consistent with a defect in the generation of COPII vesicles causing proliferation of the ER. Scale bar is 500 nm.

(Figure 2A). Protein biogenesis delays were also observed at lower temperature for the Sec24p-m11 mutant (30°C; Supplementary Figure S1A) and for the Sec24p-R230,235A B-site mutant that is defective in packaging the fusogenic SNARE, Bet1p, whereas the Sec24p-W897A A-site mutant showed no such defects (Supplementary Figure S1B). Since CPY and Gas1p are recruited into COPII vesicles by two independent cargo receptor systems, these observations were our first clue that the m11 mutation might represent a relatively severe lesion that impacts secretion in general as opposed to a cargo-specific defect. Indeed, live-cell imaging of *sec24-m11* cells expressing GFP fused to the ER resident protein, Cyb5p, revealed a dramatic expansion of the cortical ER relative to that of wild-type cells, which showed predominantly perinuclear ER fluorescence (Figure 2B). Conversely, cells expressing either the A- or B-site mutant forms of Sec24p showed normal perinuclear ER (Supplementary Figure S1C). The proliferation of internal membranes was confirmed by electron microscopy: wild-type cells showed normal perinuclear ER with several short cortical strands (Figure 2C), whereas *sec24-m11* cells accumulated abundant internal membranes, some of which were continuous with the perinuclear ER (Figure 2D). This phenotype is similar to early *sec* mutants that impair vesicle formation (Kaiser and Schekman, 1990). We consider it most likely that the m11 mutation exerts a partial and selective effect that does not induce global destabilization of Sec24p, in part because of the surface location of the lesion and in part because the mutant protein was readily expressed and purified in complex with Sec23p from yeast cells.

Sec24p-m11 causes a GTP-dependent vesicle budding defect in vitro

We tested the ability of the purified Sec23p/Sec24p-m11 complex to generate transport vesicles *in vitro* using an established reconstitution assay (Barlowe *et al*, 1994). Radiolabelled pre-pro-α-factor was translocated into microsomal membranes that were subsequently washed with urea to remove endogenous COPII proteins and then incubated with Sar1p, Sec13/31p and either wild-type Sec23/24p or Sec23p in complex with Sec24p-m11. Budding was initiated by the addition of guanine nucleotides (GDP, GTP or GMP-PNP) and the slowly sedimenting vesicle fraction was separated from the dense donor membranes by differential centrifugation. The amount of glycosylated pro-α-factor released into the vesicle fraction was quantified by Concanavalin A precipitation, and the budding efficiency calculated as the percentage of pro-α-factor in the vesicle fraction relative to that in the starting membranes. In the presence of the non-hydrolysable GTP analogue, GMP-PNP, Sec24p-m11 was able to generate COPII vesicles to a similar extent as the wild-type protein (Figure 3A); however, when GTP was included in the incubation, the budding efficiency of the Sec24p-m11 reaction was $<50\%$ of that containing wild-type Sec24p (Figure 3A). We note that the budding efficiency of wild-type reactions containing GTP is much greater than that with GMP-PNP (Figure 3A), a phenomenon that has been reported previously (Rexach and Schekman, 1991) and that likely stems from multiple rounds of coat binding, budding and release upon GTP hydrolysis. Similar experiments using a modified method that allows for immunoblotting of a range of specific cargo proteins showed similar effects: all cargo proteins that we examined were decreased in their abundance in the vesicle fraction generated by Sec24p-m11 in the presence of GTP but were relatively normal in the presence of GMP-PNP (EAM, unpublished observations). Furthermore, when Sec24p-m11 was used in a cargo-capture assay that generates pre-budding complexes, all cargoes were recruited with efficiency equal to that of wild-type Sec24p (Figure 3B), suggesting the m11 mutation does not correspond to a canonical cargo-binding motif but rather impacts vesicle formation more broadly. Thus, one explanation for a GTP-dependent budding defect is that the coat fails to turn over sufficiently to generate iterative rounds of budding.

We tested the stability of the coat generated with Sec24p-m11 using liposome binding studies that permit the hierarchical assembly of the coat on synthetic liposomes (Matsuoka *et al*, 1998). Sar1p, Sec23/24p and Sec13/31p were incubated with liposomes in the presence of GDP, GTP or GMP-PNP (Figure 3C). As expected, the coat failed to assemble in the presence of GDP, whereas GMP-PNP permitted binding of each component to the liposome, regardless of the form of Sec24p included. Similarly, the GTP-containing incubation yielded relatively poor binding of the whole coat, consistent with rapid GTP hydrolysis and coat turnover during the course of the incubation. The presence of the Sec24p-m11 mutant had no stabilizing effect and showed the same limited coat assembly as the wild-type incubation. We confirmed that the Sec24p-m11 mutant did not support stable coat assembly using a light-scattering assay that monitors coat binding and release in real time (Figure 3D), which showed wild-type and mutant Sec24p with similar kinetics of coat assembly and disassembly. Consistent with these findings, the Sec24p-m11 mutant did not have any effect on the Sec23p- and Sec31p-stimulated GTPase activity of Sar1p when monitored either by tryptophan fluorescence (EAM, unpublished observations) or by a ^{33}P-GTP hydrolysis assay (see Figure 5). Our combined biochemical analyses did not allow us to determine the molecular function of the m11 site, so we undertook a genetic approach to gain better insight into the cellular pathways that are influenced by this mutation *in vivo*.

Genetic analysis of the sec24-m11 mutant by synthetic dosage lethality screening

We used an approach known as synthetic dosage lethality (SDL; Kroll *et al*, 1996) to search for genetic backgrounds in which overexpression of Sec24p-m11 is toxic. We placed *SEC24* and *sec24-m11* under the control of a Cu^{2+}-inducible promoter, and systematically introduced these plasmids into the haploid deletion collection (Reid *et al*, 2011). Expression of *SEC24* or *sec24-m11* was induced by transfer to Cu^{2+}-containing medium and strain growth was scored using ScreenMill software (Dittmar *et al*, 2010). Strains exhibiting slow growth (*P*-value significance <0.02) when expressing an empty plasmid were discarded as likely off-target mutants that cannot tolerate the high concentrations of Cu^{2+} required to induce expression. The remaining SDL hits were further filtered to exclude strains that were affected by overexpression of both *SEC24* and *sec24-m11*. The final analysis yielded 131 strains that were specifically impaired in their ability to tolerate overexpression of the mutant protein (Supplementary Table S1). Of these, a large proportion (50 in total) were known genes involved in ER or Golgi function, or were uncharacterized components that reside in the ER or Golgi. We retested the overexpression lethality associated with the m11 mutant in these strain backgrounds and confirmed 40 validated hits (Supplementary Figure S2).

The majority of *m11*-specific hits function in various aspects of Golgi vesicle formation or fusion, and the bulk of these mutants have previously been defined as having negative genetic interactions with a hypomorphic allele of *sec24* (Schuldiner *et al*, 2005). Of particular interest to our focus on vesicle formation in the ER, was *sed4*, which had not been previously identified as showing a genetic interaction with *SEC24*, although genetic interactions with other early secretory components such as *SAR1* and *SEC16* have been defined (Gimeno *et al*, 1995; Saito *et al*, 1999). Sed4p is an integral ER membrane protein with homology to the Sar1p guanine nucleotide exchange factor (GEF), Sec12p, but lacking any GEF activity (Saito-Nakano and Nakano, 2000), and with poorly defined function (Saito-Nakano and Nakano, 2000; Kodera *et al*., 2011). We confirmed the specificity of the *sec24-m11* SDL with *sed4*Δ by placing *SEC24* under the control of the *GAL1* promoter and testing the effect of the *m11*, A-, B- or C-site mutations. Wild-type cells tolerated overexpression of all forms of *SEC24*, whereas the *sed4*Δ strain was specifically sensitive to expression of the *sec24-m11* allele (Figure 4A; LK, unpublished data). Similarly, we tested true synthetic lethality of a *sed4*Δ null mutation combined with various alleles of *SEC24*. Only the *sec24-m11* mutant was unable to grow in a *sed4*Δ strain whereas cargo-binding alleles of *SEC24* were viable in this background (Figure 4B). These genetic interactions suggest

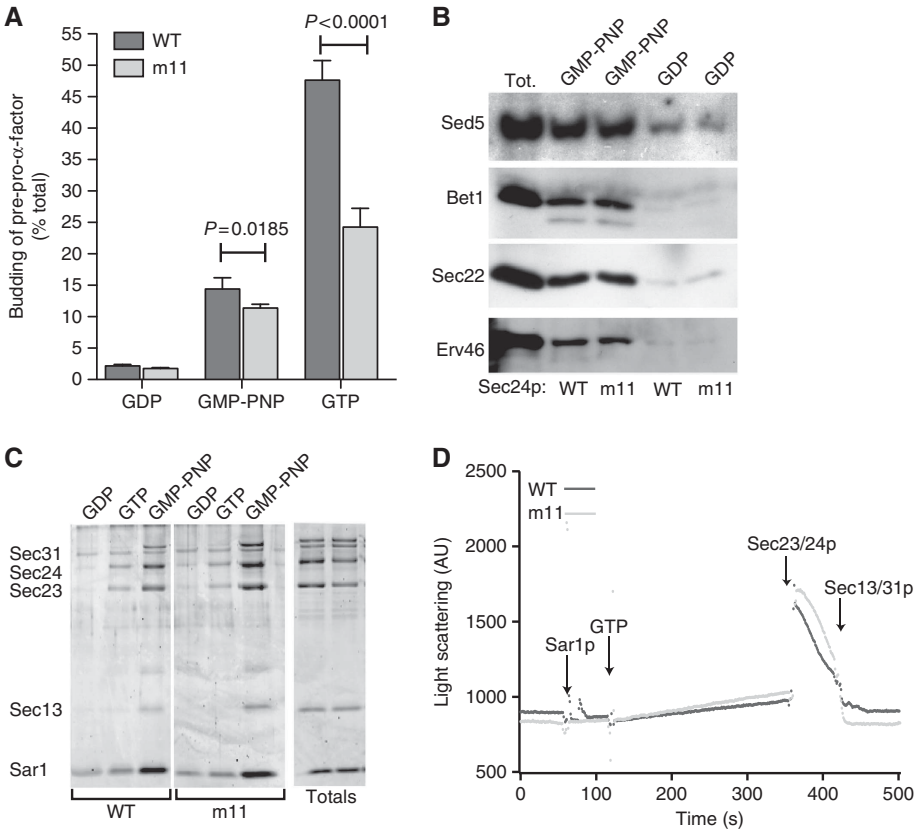

Figure 3 *In-vitro* defects in GTP-dependent vesicle formation are associated with the m11 mutation. (**A**) *In-vitro* formation of COPII vesicles was quantified by measuring release of radiolabelled pro-α-factor into a slowly sedimenting vesicle fraction following incubation at room temperature with the COPII coat supplemented with either wild-type Sec24p or Sec24p-m11. Reactions performed in the presence of GMP-PNP showed a subtle but significant difference between wild-type and m11 mutant reactions, whereas the presence of GTP caused a highly significant reduction in the budding of pro-α-factor in reactions containing Sec24p-m11. Error bars represent standard deviation from 4 to 6 independent experiments; statistical analysis was an unpaired *t*-test. (**B**) Cargo selection into pre-budding complexes was tested by incubating urea-washed microsomal membranes with GST–Sar1p and either wild-type Sec23/24p or Sec23/Sec24p-m11 as indicated. Membranes were solubilized and subjected to glutathione affinity precipitation followed by immunoblotting for the cargo proteins indicated. Sec24p-m11 permitted recruitment of all cargoes in a nucleotide-dependent manner. Tot represents 2% of the total microsomal membranes that initiated the reaction. (**C**) Coat assembly was assessed using a liposome flotation assay. COPII components were incubated with synthetic liposomes in the presence of wild-type Sec24p or Sec24p-m11 as indicated. Binding reactions were mixed with sucrose and overlaid with additional sucrose layers prior to centrifugation and collection of the floated material. Liposomes and bound proteins recovered from the top of the gradient were detected by SDS–PAGE and SYPRO red staining. The coat assembled normally with both wild-type and m11 forms of Sec24p, with stable recruitment only detected in the GMP-PNP reaction. (**D**) Coat assembly on the surface of synthetic liposomes was monitored in real time by light scattering. Recruitment of coat components to the surface of the liposome induces an increase in the light scattering signal. In the presence of GTP, this assembly is transient as the coat binds and falls apart. There was no difference in the recruitment or release of the coat when reactions containing wild-type Sec24p and Sec24p-m11 were compared.

that cells expressing the Sec24p-m11 mutant are impaired in a cellular process that also involves Sed4p; in the absence of normal Sec24p activity, a functional copy of Sed4p is required to maintain viability. The molecular function of Sed4p is not understood and appears to be specific for *S. cerevisiae* and closely related species since no obvious orthologue has been identified in more distant species. Overexpression of *SED4* suppresses the lethality associated with mutations in either *SEC16* or *SAR1* (Gimeno *et al*, 1995; Saito *et al*, 1999). These genetic interactions coupled with the fact that the cytoplasmic domain of Sed4p binds to the C-terminal domain of Sec16p suggests that it acts in conjunction with Sec16p to modulate the function of Sar1p (Gimeno *et al*, 1995; Saito *et al*, 1999; Saito-Nakano and Nakano, 2000; Kodera *et al*., 2011). Orthologues of Sec16p have been characterized in higher eukaryotes and their role in COPII vesicle formation is well established (Watson *et al*, 2006; Bhattacharyya and Glick, 2007; Iinuma *et al*, 2007; Hughes *et al*, 2009), although the exact molecular function remains unknown, which led us to test whether the *sec24-m11* mutant showed similar genetic interactions with a *sec16* mutant. Sec16p is an essential protein and is therefore not represented in the haploid deletion collection used in our SDL screen. Therefore, we tested a temperature-sensitive mutant of *sec16*, which carries a Leu-Pro substitution in residue 1088 (Espenshade *et al*, 1995) for a genetic interaction with *SEC24*. When Sec24p-m11 was the sole copy of Sec24p in a *sec16-2* background, cells were unable to grow at the normally permissive temperature of 25°C (Figure 4B). This synthetic lethality was not observed with the canonical cargo-binding mutants of Sec24p (Figure 4B), suggesting a unique feature of the m11 mutant is a perturbation in Sed4p/Sec16p-mediated regulation of vesicle budding.

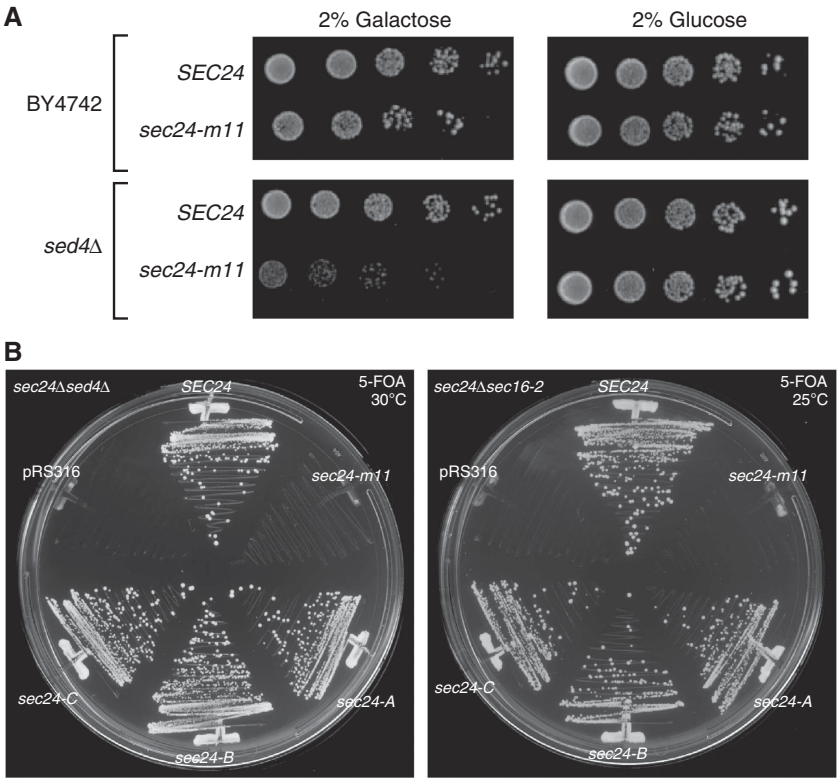

Figure 4 Expression of Sec24p-m11 is toxic in *sed4*Δ and *sec16-2* strains. (**A**) Wild-type *SEC24* or *sec24-m11* was placed under the control of the inducible *GAL1* promoter and introduced into either wild-type (BY4742, upper panel) or *sed4*Δ strains (lower panel). Serial dilutions of cells were plated onto media containing galactose to induce expression. In wild-type cells, overexpression of the m11 mutant was well tolerated whereas in the *sed4*Δ strain, growth on galactose was markedly reduced when compared with that of the wild-type overexpression plasmid. (**B**) Plasmids expressing either wild-type *SEC24* or the various mutants indicated were introduced into a *sec24*Δ *sed4*Δ or a *sec24*Δ *sec16-2* double-mutant strain and the ability to confer viability tested by growth on 5-FOA at the temperatures indicated. *sec24-m11* was unable to support viability in either strain background, whereas each of the cargo-binding mutants supported viability to a similar extent as the wild-type protein.

Sec16p delays the GTP cycle of the COPII coat, dependent on the m11 site of Sec24p

Sec16p binds to multiple components of the COPII coat and plays an essential role *in vivo* in regulating vesicle formation; yet, its precise molecular function remains unclear. However, *in-vitro* vesicle budding assays from membranes stripped of Sec16p show a defect similar to that observed with the m11 mutant of Sec24p: budding is reduced in the presence of GTP but proceeds normally with GMP-PNP (Supek *et al*, 2002). It has been postulated that Sec16p regulates the GTPase cycle of the COPII coat, but full-length Sec16p has no effect on the GTPase activity of Sar1p, as measured in a radioactive ^{32}P-GTP hydrolysis assay (Supek *et al*, 2002). Similarly, using a real-time tryptophan fluorescence assay to monitor the GDP/GTP state of Sar1p, we observed no effect of Sec16p in the conversion of Sar1p from the GTP-bound state to the GDP-bound state (Supplementary Figure S3A). However, when smaller fragments of Sec16p were tested in this assay, we discovered a dramatic effect on the rate of GTP hydrolysis by Sar1p associated with a truncated version of Sec16p that lacks the N-terminal domain. Sec16p-ΔN markedly reduced the Sec23/24p- and Sec13/31p-stimulated GTPase activity of Sar1p in a concentration-dependent manner (Figure 5A). Further dissection of the domains required for this activity yielded less clear results: a fragment encompassing residues 565–1235, which interacts with Sec24p, Sec13p and Sec31p and contains part of the ancestral coat element (ACE) domain, displayed partial GAP inhibitory function (Figure 5B); a C-terminal fragment corresponding to residues 1645–2194, which interacts with Sec23p, retained some minimal activity, detected at only high concentrations (Supplementary Figure S3B). This result suggests that different domains on Sec16p contribute to the catalytic effect: the N-terminal domain seems autoinhibitory, with the central domain conferring the bulk of the GTPase inhibitory activity and the C-terminal domain contributing additional minor activity.

The GAP inhibitory action of Sec16p was dependent on the presence of Sec13/31p: Sec16p-ΔN had only a marginal effect on the Sec23/24p-mediated GTPase activity of Sar1p but clearly inhibited the Sec13/31p-stimulated activity in a more sensitive radioactive GTP hydrolysis assay (Supplementary Figure S3C). We therefore tested the simple hypothesis that the active fragment of Sec16p prevents recruitment of Sec13/31p to the Sar1p/Sec23/Sec24p complex. We measured coat assembly on synthetic liposomes in the presence of either full-length Sec16p (which lacks inhibitory activity) or Sec16p-ΔN. Since Sec16p binds to all components of the COPII coat, increasing the concentration of Sec16p on liposomes stimulates recruitment of both Sec23/24p and Sec13/31p (Supek *et al*, 2002) and we observed the same effect of Sec16p-mediated stimulation of coat recruitment (Figure 5C). However, in the presence of increasing concentrations of Sec16p-ΔN, recruitment of Sec23/24p was stimulated as expected but the amount of Sec31p bound decreased with

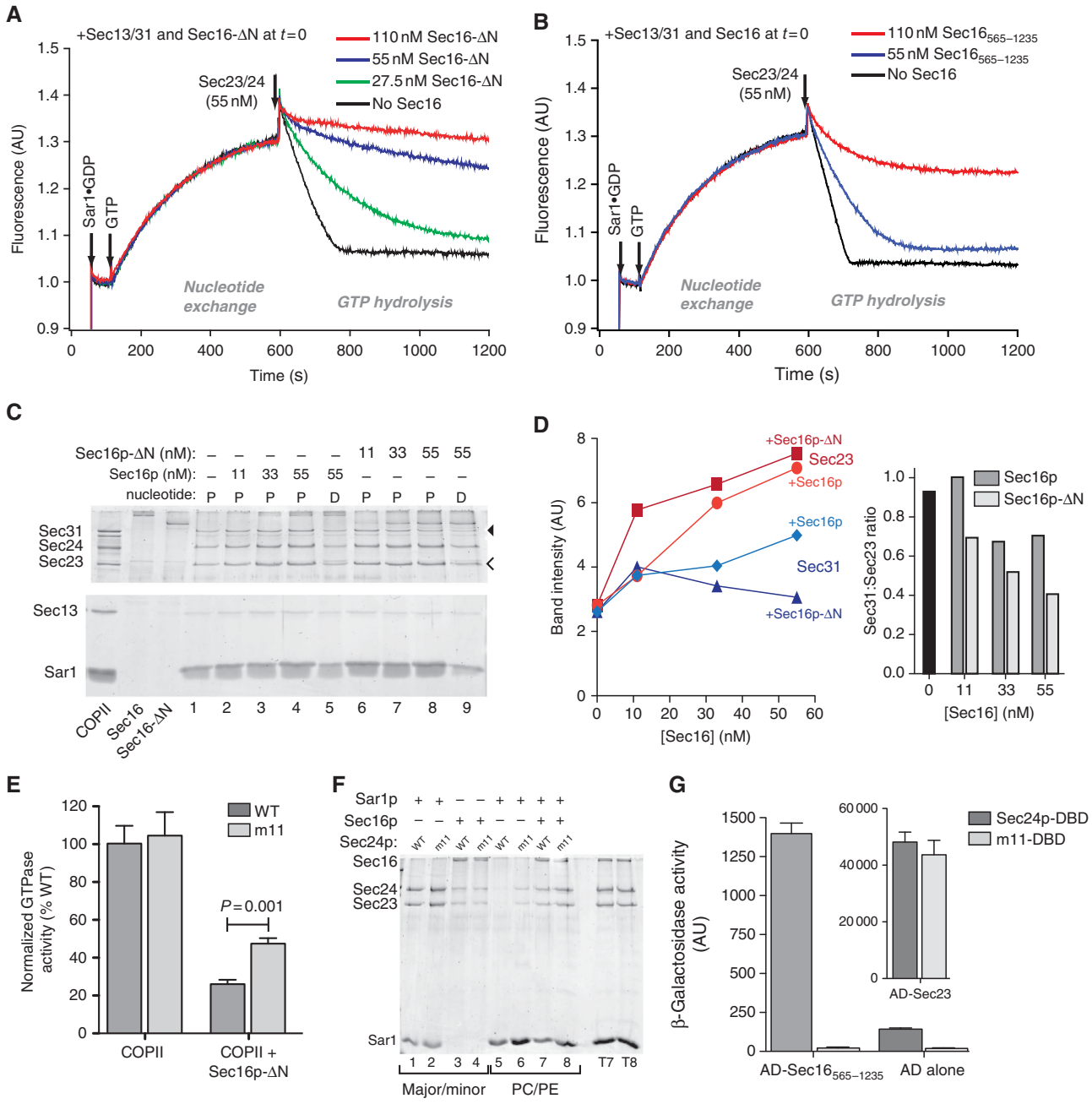

Figure 5 Sec16p-ΔN delays the GTP cycle on Sar1p, dependent on the m11 site on Sec24p. (**A**) The GTP-bound state of Sar1p (2 μM) was monitored in real time by tryptophan fluorescence in the presence of synthetic liposomes, Sec13/31p (60 nM) and different concentrations of Sec16p-ΔN. Upon GTP binding, a large increase in tryptophan fluorescence occurred, and addition of Sec23/24p (55 nM) induced rapid GTPase activity in the absence of Sec16p-ΔN. Increasing concentrations of Sec16p-ΔN reduced the conversion of Sar1p back to the GDP state, consistent with inhibition of GTPase activity. (**B**) Tryptophan fluorescence experiments using the central fragment of Sec16p, encompassing residues 565–1235 showed significant inhibition of GTPase activity on Sar1p. (**C**) Major–minor mix liposomes were incubated with COPII proteins supplemented with either full-length Sec16p or Sec16p-ΔN. Increasing concentrations of full-length Sec16p (lanes 1–4), improved the recruitment of both Sec23/24p and Sec13/31p. In contrast, increasing concentrations of Sec16p-ΔN improved Sec23/24p binding but this increase did not yield additional Sec13/31p (lanes 6–8). (**D**) Recruitment of Sar1p, Sec23p and Sec31p to COPII complexes was quantified by SYPRO Ruby staining of the liposome binding experiment shown in (**C**). In the presence of increasing concentrations of Sec16p (left panel; lighter shades), recruitment of Sec23p (red) and Sec31p (blue) increased; in incubations containing Sec16p-ΔN (darker shades), Sec23p (red) increased in liposome binding whereas Sec31p (blue) recruitment remained stable. The ratio of Sec31p to Sec23p band intensity was quantified (right panel), revealing a reduction of the Sec31p:Sec23p stoichiometry in the presence of Sec16p-ΔN. Data are representative of two independent experiments. (**E**) GTPase activity of Sar1p incubated with Sec23/24p and Sec13/31p (COPII) as determined by radioactive ^{33}P assay in the presence or absence of Sec16p-ΔN and Sec24p-m11 as indicated. Addition of Sec16p-ΔN (220 nM) dramatically inhibited the GTPase activity of Sar1p (2 μM) in the presence of Sec13/31p (60 nM) and wild-type Sec23/24p (75 nM). This effect was reduced approximately two-fold in the presence of Sec23/24p-m11. Data represent six independent experiments and error bars denote s.e.m. Statistical analysis was an unpaired *t*-test. (**F**) Sec16p-dependent recruitment of Sec23/24p to synthetic liposomes was tested in the presence and absence of Sar1p using either complex major/minor mix liposomes or simple PC/PE liposomes as indicated. No differences between wild-type Sec24p and the m11 mutant were detected, suggesting Sec16p can still form stable interactions with the Sec23/24p complex. (**G**) Interaction between Sec24p and Sec16p was monitored using a yeast two-hybrid assay where Sec24p was fused to a DNA-binding domain (DBD) and tested for interaction with Activation Domain (AD) fusions with either Sec23p (inset) or a fragment of Sec16p encompassing residues 565–1235. The m11 mutation did not alter the ability of Sec24p to interact with Sec23p but dramatically perturbed the Sec16p interaction. The data depict averages from four independent transformants and error bars represent standard deviation.

increasing Sec16p-ΔN (Figure 5C). Thus, the ratio of Sec31p to Sec23p decreased substantially as more Sec16p-ΔN was added (Figure 5D); less Sec31p recruitment to the Sar1p●Sec23p complex likely explains the reduction in GTPase activity associated with Sec16p-ΔN.

Given the genetic interaction between *sec24-m11* and *sec16-2* and their shared GTP-dependent vesicle budding defects, we tested whether the m11 mutation in Sec24p abrogated the ability of Sec16p-ΔN to modulate the GTPase activity of the COPII coat. Indeed, when Sec23p/Sec24p-m11 replaced wild-type Sec24p in the GTPase assay, the magnitude of the Sec16p-ΔN GTPase inhibition was significantly less than that observed in the presence of wild-type Sec24p, although Sec16p-ΔN still conferred some reduction in GTP hydrolysis (Figure 5E). We tested whether the Sec24p-m11 mutant is impaired in its interaction with full-length Sec16p using a liposome recruitment assay and observed no defects in the ability of Sec23/24p-m11 to be recruited to liposome-bound Sec16p under multiple conditions, with the mutant complex showing similar binding to the wild-type protein (Figure 5F). Similar results were observed with Sec23/24p-m11 recruitment to Sec16p-ΔN liposomes (SP, unpublished data). One concern with these assays is that multiple sites of Sec16p interaction may support liposome binding. In particular, Sec23p binds to the C-terminal domain of Sec16p (Gimeno *et al*, 1996) and this interaction may suffice to recruit Sec23/24p to the surface of a liposome. We therefore used yeast two-hybrid analysis to test the ability of the m11 mutation to perturb interaction between Sec24p and a smaller fragment of Sec16p that does not bind to Sec23p (Gimeno *et al*, 1996). Wild-type Sec24p gave a positive interaction with a region of the conserved central domain of Sec16p, encompassing residues 565–1235, whereas Sec24p-m11 showed no interaction with this fragment, despite interacting with Sec23p to the same extent as wild-type Sec24p (Figure 5G). These data suggest that the m11 mutation disrupts a specific interaction between Sec24p and a central region of Sec16p that contains the bulk of the GTPase inhibitory activity associated with Sec16p-ΔN. Coupled with our observation that the GTPase regulatory effect of Sec16p-ΔN is reduced in the presence of Sec24p-m11, we suggest that a Sec24p–Sec16p interaction mediated by the m11 site may coordinate the function of Sec16p in delaying the GTP cycle of the COPII coat.

Sec24p-m11 generates small vesicles and increases the stability of ER exit sites

The fact that Sec24p-m11 was defective for the inhibition of the GTPase activity conferred by Sec16p-ΔN provided us with the unique opportunity to study, both *in vitro* and *in vivo*, the effect of increased GTP hydrolysis on COPII vesicle biogenesis. We first examined the morphology of vesicles generated *in vitro* with either wild-type Sec24p or Sec24p-m11. The donor membranes retain Sec16p and thus should at least partially recapitulate the effect of the m11 mutation *in vivo*. Vesicles generated with the m11 mutant were significantly smaller than those generated with the wild-type coat (Figure 6A and B). This observation is consistent with emerging models that suggest GTP hydrolysis on Sar1p and the coincident rearrangement of its amphipathic N-terminal helix are required for the vesicle scission event that releases a mature COPII vesicle from the donor membrane (Bielli *et al*, 2005; Lee *et al*, 2005). Increased or premature GTP hydrolysis in the presence of Sec24p-m11 would thus drive release of immature small vesicles that contain less membrane, explaining the expanded donor ER membranes observed by EM and fluorescence microscopy (Figure 2). Furthermore, this structural defect in vesicle biogenesis could cause the inefficient packaging of cargo proteins described in Figure 3.

We next visualized the dynamics of the COPII coat *in vivo* in strains expressing the Sec24p-m11 mutant as the sole copy of Sec24p where the chromosomal copy of *SEC13* had been fused in-frame with monomerized GFP (Snapp *et al*, 2003). We examined turnover of Sec13p–GFP on ER exit sites using Fluorescence Loss in Photobleaching (FLIP) to alternately photobleach a region of interest and then image the whole cell (Ellenberg *et al*, 1997). Photobleaching one region of the cell depletes visible Sec13p from ER exit site structures within that region as well as cytoplasmic Sec13p that freely diffuses through the area of photobleaching (Figure 6C). Since Sec13p is also a subunit of the nuclear pore complex, we excluded the nuclear envelope from the fluorescence loss analysis, although similar results were obtained using whole-cell data. Mean Sec13p–GFP fluorescence was higher in cells expressing Sec24p-m11 (Figure 6E, inset), likely due to the expansion of the ER membrane creating additional tER sites (Figure 2). Furthermore, the pixel variance across individual cells was also significantly higher in the mutant relative to wild type (Figure 6D). This measure is an indicator of cellular distribution: small pixel variance corresponds to a relatively homogeneous distribution of brightness across the cell whereas high pixel variance occurs where cells display distinct bright spots in a dim surrounding environment. These measurements suggest that in the *sec24-m11* strain the coat is tightly associated with ER exit sites with relatively less fluorescence in the diffuse cytoplasmic pool (i.e., a more heterogeneous distribution and therefore higher pixel variance), contrasted with a more even distribution between ER exit sites and cytosol (and therefore lower variance) in wild-type cells. The kinetics of Sec13p–GFP turnover reinforce this interpretation; loss of coat fluorescence was less in the *sec24-m11* strain (Figure 6D) with the half-life of the total extranuclear fluorescence significantly longer than in wild-type cells (Figure 6E), suggesting a tighter association of Sec13p–GFP at ER exit sites and less protein entering into the freely diffusible (and thus bleachable) pool. Such a distribution of Sec13p–GFP within a stable ER exit site that is liberated less quickly into the diffusible recycling pool is consistent with the release of small vesicles from the ER: during each round of budding, less coat is removed from the relatively stable ER exit site pool leading to less coat release into the cytoplasm as the vesicle is consumed.

Together, our data suggest that the Sec24p-m11 mutation results in heightened GTPase activity of the COPII coat, the effect of which is premature release of small vesicles and a reduction in coat turnover. These findings shed new light on the functional role of GTP hydrolysis by the COPII coat, and suggest a surprising function for Sec24p in modulating this process.

Discussion

It has long been recognized that the GTP cycle of the COPII coat plays a fundamental role in permitting forward traffic.

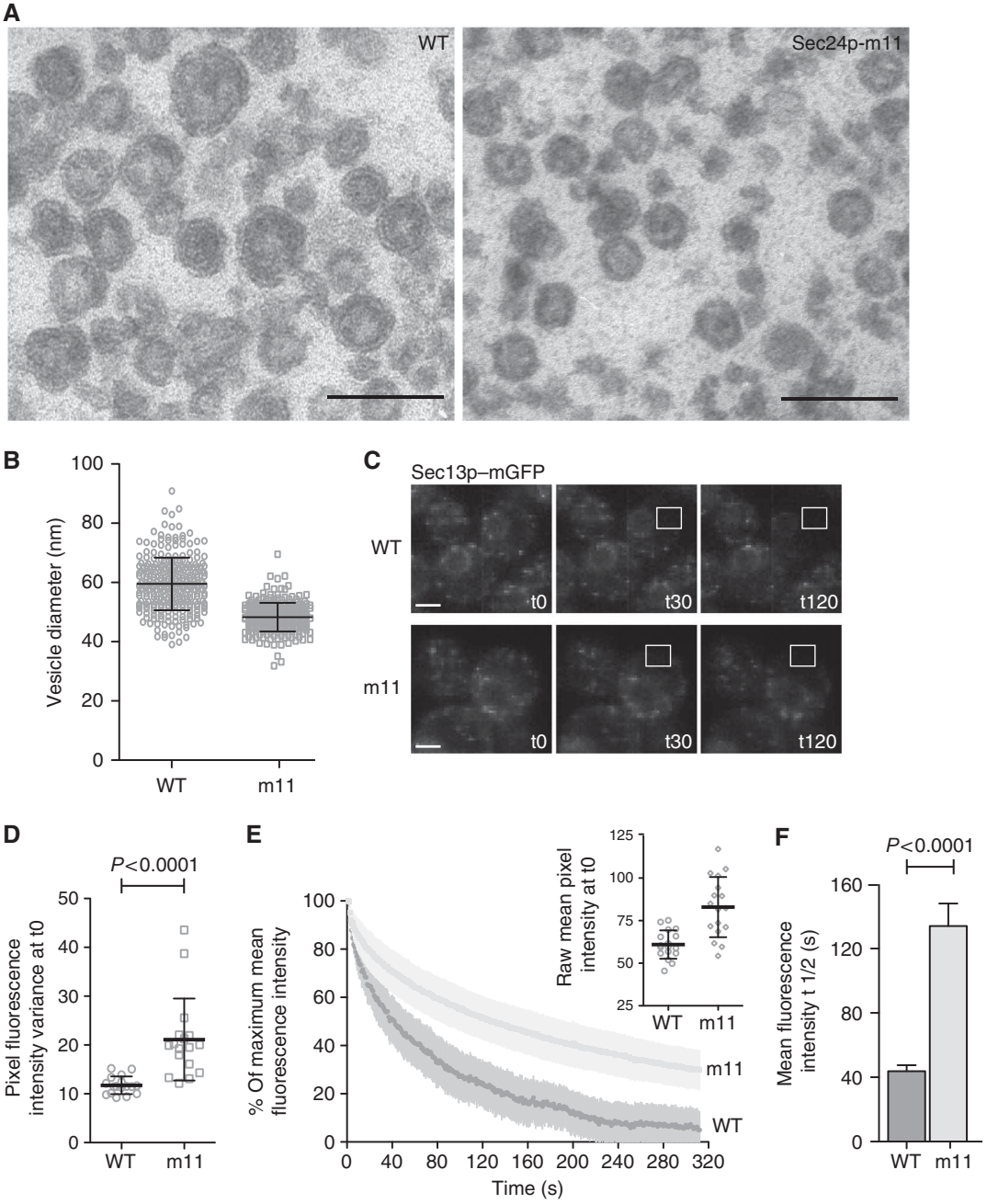

Figure 6 Sec24p-m11 generates small vesicles and increases the lifetime of the coat on ER exit sites. (**A**) Microsomal membranes were urea washed to remove endogenous coat proteins and incubated with Sar1p (10 μg/ml), Sec13/31p (20 μg/ml) and either wild-type Sec23/24p (10 μg/ml) or Sec23/Sec24p-m11 (10 μg/ml) as indicated in the presence of GTP. Vesicles were separated from donor membranes in a medium speed centrifugation and fixed for thin section electron microscopy. Scale bar represents 100 nm. (**B**) The diameters of ~250 vesicles from each treatment were measured, revealing that the wild-type vesicles (59.5 nm) were significantly larger than the m11 vesicles (48.3 nm), $P<0.0001$. Individual measurements are plotted, along with population means; error bars represent s.d. and statistical analysis was an unpaired *t*-test. (**C**) Images of wild-type and *sec24-m11* cells expressing Sec13p–mGFP before (t0, left panels) and at various times during repetitive photobleaching experiments, where the region of photobleaching is outlined by the white box. Scale bar is 2 μm. (**D**) Pixel variance, which represents the spread of pixel intensities across an individual cell, was significantly greater in the *sec24-m11* mutant strain, suggesting a tighter distribution of Sec13p-mGFP in bright punctae as opposed to a more homogeneous or diffuse distribution in wild-type cells. Individual measurements are plotted along with population means; error bars represent s.d. and statistical analysis was an unpaired *t*-test ($n=17$). (**E**) Normalized fluorescence intensity was plotted over time, revealing a significant difference between wild-type (WT) and *sec24-m11* mutant. Mean and standard deviation are plotted for each time point ($n=17$). The raw mean fluorescence intensity at the start of the experiment was greater for the mutant relative to wild type (inset) with individual measurements plotted and mean and standard deviation indicated. (**F**) The half-time of mean cellular fluorescence decay was markedly increased in the *sec24-m11* cells, suggesting less turnover of the coat in these mutants. Mean ± s.e.m. is plotted; statistical analysis was an unpaired *t*-test ($n=17$).

The predominant view has been that GTP hydrolysis by Sar1p functions primarily in vesicle uncoating, which is required for exposure of the docking and fusion machineries that drive membrane mixing at the Golgi. In support of this model, vesicles generated *in vitro* with non-hydrolysable GTP analogues retain their coat and cannot undergo fusion, whereas

vesicles generated with GTP rapidly lose their coat, although the extent of coat loss varies with different methods of vesicle purification (Barlowe *et al*, 1994). Thus, the catalytic cycle of the COPII coat has been viewed primarily as one of coat recruitment and stability on the membrane. The discovery that the inner and outer layers of the COPII coat, specifically Sec23p and Sec31p, conspire to maximally stimulate GTP hydrolysis by Sar1p (Antonny *et al*, 2001), established a paradox for vesicle formation: how are transport carriers generated when full assembly of the coat triggers its own demise?

Given the intrinsic instability of the purified coat, additional players have been postulated to influence the process of coat assembly, and for a number of years, Sec16p has been a prime candidate as a coat regulator by virtue of its genetic and physical associations (Espenshade *et al*, 1995; Gimeno *et al*, 1996; Shaywitz *et al*, 1997). However, when Sec16p was finally purified, it had no effect on the GTP cycle of the COPII coat but instead seemed to function as a scaffold to promote recruitment of all the COPII subunits (Supek *et al*, 2002). We have now demonstrated that a fragment of Sec16p can in fact modulate the GTP cycle of the COPII coat, and we note that a construct encoding this truncated protein (encompassing residues 565–2194) was originally observed to complement a *sec16-Δ1* null strain, consistent with a fundamental role for Sec16p-ΔN in preserving cellular function *in vivo* (Espenshade *et al*, 1995). Since full-length Sec16p clearly lacks GTPase inhibitory activity, we propose that the N-terminal region (residues 1–565) is an autoinhibitory domain that functions to antagonize GAP inhibition. Although the precise mechanism by which Sec16p-ΔN impacts GTP catalysis by Sar1p–Sec23p–Sec31p remains to be fully explored, our data suggest that the presence of this shortened version of Sec16p prevents stoichiometric recruitment of Sec31p to Sec23p, thereby reducing GAP stimulation by Sec31p. Sec16p may additionally function in a non-catalytic role as a scaffold to promote recruitment of individual COPII proteins (Gimeno *et al*, 1996; Supek *et al*, 2002), additional components like the newly defined TFG-1 (Witte *et al*, 2011) and potential regulators like Sed4p. Furthermore, Sec16p has a clear role in organizing the local environment of an ER exit site (Ivan *et al*, 2008; Hughes *et al*, 2009) dependent on its phosphorylation by ERK7 (Zacharogianni *et al*, 2011), although it remains to be seen whether this morphological role is functionally related to its action as a scaffold or modulator of the GTP cycle.

Our finding that a mutation in Sec24p also impacts the GTPase activity of the COPII coat is surprising: Sec24p functions primarily as a cargo adaptor (Miller *et al*, 2003; Mossessova *et al*, 2003), and in minimally reconstituted systems shows no evidence of a role in GTP hydrolysis (Bi *et al*, 2007). However, in the context of a GTPase reaction containing Sec16p-ΔN, there is a clear effect of the m11 mutation. Together with our yeast 2-hybrid experiments that suggest that Sec24p-m11 is impaired in its interaction with the catalytically active fragment of Sec16p, our findings raise the exciting possibility that Sec24p and Sec16p act together to coordinate GTPase activity (and vesicle release) with cargo loading. This concept of cargo 'priming' was originally postulated when the vesicle-borne SNARE, Bet1p, was found to bind to the Sar1p–Sec23p–Sec24p 'pre-budding' complex (Springer and Schekman, 1998). According to this model, cargo itself would nucleate coat assembly to ensure that vesicles are populated with adequate cargo, and in particular with the SNARE proteins that drive fusion (Springer *et al*, 1999). An extension of this model is suggested by our findings: cargo-bound Sec24p would engage Sec16p to inhibit GTPase activity and thereby delay vesicle release until sufficient cargo loading and/or coat propagation has occurred. By requiring an interaction between the cargo-binding adaptor of the coat (Sec24p) and a negative regulator of vesicle release (Sec16p), the generation of cargo-free vesicles would be avoided, freeing unoccupied coat components to undergo iterative rounds of membrane binding and release. One prediction of this model is that the GAP inhibitory function of Sec24p and Sec16p would be enhanced by the presence of cargo. We searched for such an effect of heightened GTPase inhibition in the presence of the fusogenic SNARE proteins, Bet1p and Sed5p, but were unable to detect any change in GTPase activity (LK, unpublished data). It may be that these specific molecules do not induce the GTP delay, or that a combination of diverse cargoes is required to trigger such an effect. Further characterization of the complexity of these interactions, in particular with regard to how occupancy of Sec24p with secretory cargo might allosterically regulate its interaction with Sec16p, will elucidate the molecular details of the GTPase cycle during vesicle biogenesis. Of particular interest will be relatively large cargoes like Pma1p in yeast (Lee *et al*, 2002) and collagen in mammalian cells (Malhotra and Erlmann, 2011), which likely depend on large vesicles/tubules for efficient ER export. Preventing premature vesicle scission should be key to ensuring capture of these large complexes.

One feature of the Sec24p-m11 mutant was the generation of remarkably small COPII vesicles, suggesting that the heightened GTPase activity associated with this mutation results in premature vesicle release rather than futile cycles of coat binding and disassembly. This conclusion is also supported by our experiments measuring the *in-vivo* dynamics of the COPII coat in the presence of the Sec24p-m11 mutant: we observed an increase in the lifetime of Sec13p–GFP at ER exit sites rather than a decrease, which would be expected if the enhanced GTPase activity resulted in rapid coat disassembly. These findings are consistent with emerging models that suggest that coat stability is not a simple product of the GTPase activity of the Sar1p–Sec23p–Sec31p complex. First, the GTP cycle of the COPII coat and subsequent coat stability is influenced by the ER-localized GEF, Sec12p, which prolongs coat association on synthetic liposomes by feeding additional Sar1p into the system (Futai *et al*, 2004; Sato and Nakano, 2005). Furthermore, the presence of cargo proteins also increases the lifetime of the coat on synthetic lipid bilayers, permitting membrane association of Sec23/24p even after Sar1p has completed GTP hydrolysis (Sato and Nakano, 2005). That Sec23/24p stably associates with cargo-containing membranes is consistent with recent findings that implicate vesicle-bound Sec23p in the tethering activity of the TRAPP complex to regulate directionality of COPII vesicle delivery: prolonged association of Sec23/24p on the vesicle, perhaps by virtue of an association with cargo proteins, marks the vesicle for interaction with the TRAPP complex to initiate docking with the Golgi acceptor membrane (Cai *et al*, 2007; Lord *et al*, 2011). Thus, a mounting body of evidence suggests that on cargo-containing

membranes, the COPII coat is relatively stable even after GTP hydrolysis by Sar1p and its release from the vesicle. Such a model is consistent with a fundamental role for Sar1p in vesicle release (Bielli *et al*, 2005; Lee *et al*, 2005), perhaps via destabilization of the lipid bilayer (Settles *et al*, 2010) and explains the absence of a dynamin-like scission machine for the COPII coat (Pucadyil and Schmid, 2009). Our findings suggest that Sec16p functions in part to delay vesicle release, perhaps coupled via Sec24p with cargo loading of the nascent vesicle such that only a mature vesicle, replete with cargo, will be liberated from the ER.

Materials and methods

Yeast growth, strains and plasmids

Standard yeast growth conditions and transformation protocols were used. Cultures were grown at 25°C (for temperature-sensitive strains) or 30°C either in rich medium (YPD: 1% yeast extract, 2% peptone, 2% glucose) or in synthetic complete medium (SC: 0.67% yeast nitrogen base, 2% glucose, supplemented with amino acids as required). Complementation analysis was performed by streaking transformants onto selective medium supplemented with 5-fluoroorotic acid (5-FOA: 0.1% final concentration). Strains and plasmids are listed in Table I. To generate new *sec24*Δ double mutants, *SEC24* was deleted in the YPH499 background by PCR-mediated integration of a *sec24*Δ*::NATMX* cassette into a strain carrying *SEC24* on a *URA3*-marked plasmid (pLM22) to create LKY022. The *sec24*Δ *sed4*Δ and *sec24*Δ *sec16-2* double mutants were generated by standard genetic crosses between LKY022 and *sed4*Δ or *sec16-2* strains, respectively. The m11 mutation (E504A, D505A) was introduced into pLM23, pLM129 and pJW1512-SEC24 by QuikChange site-directed mutagenesis (Stratagene). Full-length and N-terminally truncated Sec16p genes were amplified from yeast genomic DNA using primers that incorporated a 10 × His tag at the 5′ end of the gene. PCR products were cloned into a pCR-Blunt-TOPO vector (Invitrogen), confirmed by sequencing and subcloned into the *Bam*HI and *Xho*I sites of the p426GAL vector for galactose-mediated overexpression in yeast (Mumberg *et al*, 1994). The central (residues 565–1235) and C-terminal (residues 1645–2194) domains of Sec16p were amplified from yeast genomic DNA using primers that incorporated an N-terminal 10 × His tag and 5′ and 3′ *Bam*HI sites. These PCR products were cloned into the *Bam*HI site of pGEX2T (GE Healthcare) for expression in *E. coli*. *SEC24* was

Table I Strains and plasmids

Strain	Genotype	Source
RSY620	*MATα leu2-3,112 ura3-1 can1-100 ade2-1 trp1-1 his3-11,15 pep4::TRP1*	Schekman laboratory
YPH499	*MAT**a** ura3-52 lys2-801_amber ade2-101_ochre trp1-Δ63 his3-Δ200 leu2-Δ1*	Sikorski and Hieter (1989)
YTB1	*MATα can1-100 leu2-2,112 his3-11,15 trp1-1 ura3-1 ade2 sec24::LEU2* carrying pLM22 (CEN SEC24-URA3)	Miller *et al* (2003)
YTB20	*MATα can1-100 leu2-2,112 his3-11,15 trp1-1 ura3-1 ade2 sec24::LEU2 iss1::KanR* carrying pLM22 (CEN SEC24-URA3)	Miller *et al* (2003)
BY4742	*MATα his3Δ1 leu2Δ0 lys2Δ0 ura3Δ0*	Open Biosystems
LMY864	*MAT**a** ura3-52 lys2-801_amber ade2-101_ochre trp1-Δ63 his3-Δ200 leu2-Δ1 sec24::NATMX* carrying pLM22 *(CEN SEC24-URA3)*	This study
sed4Δ	*MATα his3Δ1 leu2Δ0 lys2Δ0 ura3Δ0 sed4Δ::KanR*	Open Biosystems
LKY024	*MAT**a** ura3 lys2 ade2 trp1 his3 leu2 sec24Δ::NATMX sed4Δ::KanR* carrying pLM22 *(CEN SEC24-URA3)*	This study
RSY267	*MATα his4-619 ura3-52 sec16-2*	Schekman laboratory
LKY026	*MAT**a** ade2 ura3 leu2 his3 trp1 lys2 sec24Δ::NatMX sec16-2* carrying pLM22 *(CEN SEC24-URA3)*	This study
W7620-3C	*MAT**a** trp1-1 his3-11,15 leu2-3,112 ura3-1 ade 2-1 rad5-535 lys2Δ met17Δ CEN1-16:: Gal-Kl-URA3*	Rothstein laboratory
FSY9	*MAT**a**/α ade2-1/ADE2 his3-11,15/his3-Δ200 leu2-3,112/leu2-Δ1 LYS2/lys2-801am ura3-1/URA3 trp1-Δ1/trp1 PRB1/prb1Δ1.6R pep4::TRP/pep4::HIS3 SEC16/SEC16:: KAN-CUP1pr-MalE*	Supek *et al* (2002)
LMY238	LMY864 with *SEC13-mGFP::TRP1* carrying pLM23 (*CEN SEC24-HIS3*)	This study
LMY239	LMY864 with *SEC13-mGFP::TRP1* carrying pLM22 *(CEN sec24-m11-HIS3)*	This study

Plasmid	Description	Source
pLM22	4.2 kb *Xho*I–*Spe*I fragment containing 6 × His-tagged *SEC24* in pRS316	Miller *et al* (2003)
pLM23	4.2 kb *Xho*I–*Spe*I fragment containing 6 × His-tagged *SEC24* in pRS313	Miller *et al* (2003)
pLM148	*sec24-m11* (E504A, D505A) mutation in pLM23	This study
pLM129	2.8 kb *Xba*I–*Hin*dIII fragment containing 6 × His-tagged *SEC24* in p425GAL1	Miller *et al* (2003)
pLM161	*sec24-m11* (E504A, D505A) mutation in pLM129	This study
pTKY9	*SEC23* in p426GAL1	Kurihara *et al* (2000)
pLM251	*sec24-a4* (W897A) mutation in pLM23	Miller *et al* (2005)
pLM134	*sec24-b3* (R230, R235A) mutation in pLM23	Miller *et al* (2003)
pLM174	*sec24-c1* (R342A) mutation in pLM23	Miller *et al* (2003)
GFP–Cyb5	MET25pr–GFP–CYB5 (CEN URA3)	Beilharz *et al* (2003)
pEG202	lexA DNA binding domain in a 2-μ *HIS3*-marked vector	Gyuris *et al* (1993)
pSH18-34	lacZ reporter gene in a 2-μ *URA3*-marked vector	Gyuris *et al* (1993)
pPE81	*SEC23* in pJG4-5 (acidic activation domain in a 2-μ TRP1-marked vector)	Espenshade *et al* (1995)
pPE167	*SEC16* (565–1235) in pGAD-GH	Gimeno *et al* (1995)
pRH286	*SEC24* (34–926) in pEG202	Gimeno *et al* (1995)
pLK125	E504AD505A mutation introduced into pRH286	This study
p426GAL-Sec16	Full-length Sec16p with N-terminal 10 × His tag in p426GAL1	This study
p426GAL-Sec16ΔN	Sec16-ΔN (residues 565–2194) with N-terminal 10 × His tag in p426GAL1	This study
pGEX-Sec16Cen	Central fragment of Sec16 (residues 565–1235) with N-terminal 10 × His tag in pGEX2T	This study
pGEX-Sec16Cter	C-terminal fragment of Sec16 (residues 1645–2194) with N-terminal 10 × His tag in pGEX2T	This study
pJW1512	CUP1pr CEN LEU3	Reid *et al* (2011)
pJW1512-SEC24	CUP1pr-SEC24 in pJW1512	This study
pJW1512-sec24m11	*CUP1pr-SEC24-m11* (E504A, D505A) in pJW1512	This study

placed under the control of the *CUP1* promoter by *in-vivo* gap repair of a PCR-generated product into the gapped plasmid pJW1512 (Reid *et al*., 2011), and the m11 mutation introduced by QuikChange mutagenesis (Stratagene).

Pulse-chase analysis

To examine secretory pathway function in the presence of various *SEC24* mutants, YTB1 (*sec24*Δ, carrying *pSEC24-URA3*) was transformed with wild-type *SEC24* (pLM23), or the various mutants (pLM148, pLM251, pLM134 or pLM174 corresponding to the m11, A-, B- and C-site mutants. respectively), followed by counter-selection on media containing 5-FOA to remove the wild-type *URA3*-containing version of *SEC24*. These strains were subjected to pulse-chase analysis as described (Pagant *et al*, 2007) using Gas1p- and CPY-specific antibodies.

Fluorescence and electron microscopy

To examine the morphology of the endoplasmic reticulum by fluorescence microscopy, a plasmid encoding the ER membrane protein, Cyb5p, fused to GFP (Beilharz *et al*, 2003) was introduced into strains expressing wild-type or mutant forms of *SEC24* as the sole copy of *SEC24* (described above in the section on pulse-chase analysis). Transformants were grown in SD-ura at 30°C, shifted to 37°C for 1 h and examined using a Nikon Ti-E inverted microscope with × 100 NA 1.4 PlanApo optics and a CoolSnap HQ2 camera. Images were collected with Nikon NIS Elements software and assembled using Adobe Photoshop (Adobe Systems). To visualize cellular morphology at high resolution, cells were grown at 30°C in rich medium, transferred to 37°C for several hours prior to fixation and processing for transmission electron microscopy as described (Kurihara *et al*, 2000). Thin section electron microscopy of vesicle preparations was prepared as described (Miller *et al*, 2002). FLIP experiments were performed at 25°C on a Zeiss Duoscan confocal microscope with a × 63 NA 1.4 oil objective and a 489-nm 100 mW diode laser with a 500–550 nm bandpass filter. For FLIP experiments, a small region of interest was repetitively bleached and total cellular fluorescence imaged over time as described (Lai *et al*., 2010). Fluorescence intensity and pixel standard deviation (s.d.) were measured using *ImageJ* (NIH) software and statistical analysis performed with Prism 5.0 (GraphPad Software). Images were collected and assembled using Adobe Photoshop and Adobe Illustrator (Adobe Systems).

Protein purification

Sar1p and Sec13/31p were purified as previously described (Barlowe *et al*, 1994). Sec23/24p was purified following galactose-induced overexpression as described (Miller *et al*, 2003). Full-length Sec16p was purified either as described (Supek *et al*, 2002), or using galactose-mediated overexpression. Plasmids expressing galactose-inducible 10 × His-tagged full-length or N-terminally truncated Sec16p were introduced into RSY620 cells. Strains were grown in non-inducing medium (SC-ura using 5% glycerol and 0.1% glucose as the carbon source) at 30°C in a 12-L fermenter (New Brunswick). At late log phase, galactose was added to a final concentration of 0.2% and cells grown for a further 6 h. Cells were collected by centrifugation, washed with water and resuspended in JR buffer (20 mM Hepes-KOH pH 7.4, 50 mM KOAc, 2 mM EDTA, 0.2 M sorbitol) to 10% of the cell weight. The cell suspension was frozen as drops in liquid nitrogen and stored at −80°C. Frozen cell beads were ground to a powder under liquid nitrogen in a Waring blender, thawed on ice and diluted with 300 ml of JR buffer containing 1 mM DTT and protease inhibitor (PI) cocktail. Unbroken cells were removed by low speed centrifugation (10 min at 500 *g* in a Sorvall GS3 rotor), and heavy membranes collected by centrifugation of the supernatant at medium speed (30 min at 17 000 *g* in a Sorvall GS3). These membranes were washed twice with buffer B88 (20 mM Hepes-KOH pH 6.8, 150 mM KOAc, 5 mM MgOAc, 0.25 M sorbitol, 1 mM DTT) supplemented with PIs prior to salt extraction of Sec16p with 30 ml of buffer EF2 (20 mM Hepes-KOH pH 7.4, 500 mM NaCl, 0.1 mM EGTA, 0.2 M sorbitol, 10% glycerol, 20 mM imidazole, 1 mM DTT, + PI) and stirring for 30 min at 4°C. The stripped peripheral proteins were recovered in the supernatant following centrifugation for 30 min at 27 000 g in a Sorvall SS34 rotor and incubated with 4 ml of Ni-NTA slurry (Qiagen) overnight at 4°C. The resin was washed sequentially with buffer EF2, EF2 supplemented with 50 mM imidazole and EF2 supplemented with 75 mM imidazole. The Ni-NTA resin was transferred to a column and Sec16p eluted with a gradient of imidazole (EF2 with 100–500 mM imidazole); fractions containing Sec16p were identified by SDS–PAGE, pooled and dialysed into buffer HK500 (20 mM Hepes-KOH pH6.8, 500 mM KOAc, 10% glycerol, 1 mM DTT). The central and C-terminal fragments of Sec16p were purified from *E. coli* as described (Parlati *et al*, 2000) with the exception that octylglucoside was excluded from the final wash and elution buffers.

In-vitro vesicle budding and liposome binding

Purified COPII proteins were used to generate vesicles *in vitro* from purified microsomal membranes as described (Miller *et al*, 2002). Briefly, ^{35}S-pre-pro-α-factor was translated *in vitro* and post-translationally translocated into microsomal membranes. Endogenous COPII proteins were removed by washing membranes with 2.5 M urea in buffer B88, followed by additional washes in B88 alone. Membranes were incubated with Sar1p, Sec13/31p and either wild-type or mutant Sec23/24p in the presence of GDP, GMP-PNP or GTP plus ATP regeneration system. Vesicles were separated from the donor membrane by medium-speed centrifugation and the amount of glycosylated pro-α-factor incorporated into the vesicle fraction was quantified by ConcanavalinA precipitation and scintillation counting. Formation of cargo-containing 'pre-budding complexes' was performed as described (Kuehn *et al*, 1998). Briefly, microsomal membranes were washed with urea then incubated with GST–Sar1p, Sec23/24p and GMP-PNP. Membranes were solubilized and bound cargoes examined by immunoblotting after glutathione affinity precipitation of the COPII complex.

Coat assembly onto synthetic liposomes was assessed as previously described (Matsuoka *et al*, 1998) using either major/minor mix liposomes or simple PC/PE liposomes as required. In the case of binding reactions containing Sec16p, the concentration of KOAc was adjusted to compensate for the high salt concentration present in the protein preparation (Supek *et al*, 2002). COPII proteins recruited to floated liposomes were detected by SDS–PAGE and SYPRO Red (Invitrogen) staining followed by quantitation of binding using a Typhoon Imager and ImageQuant software (Molecular Dynamics). Real-time analysis of coat assembly was assessed using light scattering as described (Antonny *et al*, 2001).

SDL screen

SDL screens were performed essentially as described in Reid *et al* (2011). Plasmids encoding wild-type *SEC24* and *sec24-m11* under the control of the *CUP1* promoter were transformed into the donor strain, W7620-3C. Transformants were inoculated into selective media and grown to saturation. Cultures were plated onto YPD and grown as lawns overnight at 30°C. Replica pinning steps were performed using a Singer RoToR HDA benchtop robot (Singer Instrument Company). The *MAT***a** genomic deletion library (Open Biosystems) was arrayed from a 16 × 24 grid (384 colonies) to a 32 × 48 grid (1536 colonies), with each strain represented in quadruplicate, and grown on YPD with 200 mg/ml G418 overnight. These deletion strains were pinned onto the donor strain lawns and plates were incubated for 6 h at 30°C to allow mating before counterselecting for haploid library strains carrying the plasmid of interest on SGal plates (0.67% yeast nitrogen base, 2% galactose, supplemented with amino acids appropriate for autotrophic growth). After 24 (Screen 1) or 36 (Screen 2) hours of selection, cells were replica pinned onto control SGal media with 5-FOA (0.1% final concentration) and SGal media with 5FOA and 200 mM $CuSO_4$ to induce overexpression of the plasmid-borne genes. Plates were scanned after 48, 56 or 72 h of growth and scanned images were parsed, cropped, rendered into pixels with *ImageJ* software (NIH) and the *ScreenMill* software analysis suite (Dittmar *et al*, 2010). Average colony size for each individual plate was calculated by *ScreenMill* and used to determine the statistical significance of impaired growth of colonies overexpressing *SEC24* or *sec24-m11* compared with those carrying a control plasmid. Strains that displayed a *P*-value significance of <0.02 specifically upon *sec24-m11* overexpression were considered positive hits. The screen was performed twice in order to ensure maximal coverage and positive hits from either screen were pooled to yield a total of 131 hits (Supplementary Information, Table S1), which were categorized based on function or localization. A manually selected list of 50 strains with known function in vesicle trafficking, or defined localization to either the ER or Golgi, were targeted for validation of their SDL phenotypes. The selected library strains were manually transformed with pJW1512 bearing either wild-type *SEC24* or *sec24-*

m11 using standard LiAc techniques. Transformants were grown to saturation in selective media and serial dilutions were spotted onto selective media containing 400 mM $CuSO_4$ to induce overexpression. After 2 days of growth at 30°C, the plates were scanned and the growth phenotypes were noted. Strains sensitive to overexpression of *sec24-m11*, but tolerant of wild-type *SEC24* overexpression, compared with overexpression in a BY4742 control strain were accepted as SDL hits.

Yeast two-hybrid analysis

Colorimetric β-galactoside activity assays were performed as previously described (Espenshade *et al*, 1995) with some modifications. Cells expressing the appropriate wild-type or mutant Sec24p-DBD, Sec16p-AD, and/or Sec23p-AD constructs and a reporter construct were grown in minimal media to mid-log phase (0.4–0.8 OD_{600}). For constructs requiring galactose induction, cells were grown in selective media containing 2% raffinose as the carbon source to mid-log phase and induced for 4–5 h with 0.2% galactose. Approximately 2.0–4.0 OD_{600} of cells were harvested and resuspended in 200 µl of breaking buffer (100 mM Tris, pH 8.0, 1 mM DTT, 2% glycerol) supplemented with PIs before glass bead lysis for 5 min at 4°C. The cell lysates were cleared by centrifugation at 13 000 r.p.m. for 5 min at 4°C. Lysate volumes of 5–50 µl were used in each reaction; for reactions containing <50 µl of lysate, the appropriate difference in volume was supplemented with breaking buffer. To each lysate sample, 450 µl of 2.23 mM CPRG (Chlorophenol red-b-D-galactopyranoside; Roche) in 100 mM HEPES, 150 mM NaCl, was added to initiate the reaction. Upon appearance of red product, 150 µl of 6 mM $ZnCl_2$ was added to quench the sample and the reaction time was noted. The OD_{574} was measured and the specific activity for each sample was measured by the following equation, reported in Miller units: $(OD_{574} \times 0.65)/(0.0045 \times \text{protein concentration} \times \text{volume} \times \text{time})$, where protein concentration is measured in mg/ml, volume of lysate used in ml, and time in minutes. Protein concentration of the lysates was determined by BioRad Protein Assay (Bio-Rad). Three to six independent transformants were tested for each interaction.

GTPase assays

The GTPase activity of the COPII coat was measured using either tryptophan fluorescence or a radioactive TLC-based assay as described (Antonny *et al*, 2001). For better temporal resolution, the tryptophan fluorescence assays were performed in a cylindrical cuvette (sample volume 550 µl) in which the reactions were mixed by a magnetic stir bar, and injection of COPII proteins and nucleotides was done through a Hamilton syringe. In the radioactive GTPase assays, either α-^{32}P-GTP (Supplementary Figure 3C) or α-^{33}P-GTP (Figure 5C) was used, and the rate of GTP hydrolysis was calculated by quantifying the pmol of GDP released over time. GTPase activity is represented as the pmol GDP released per second. Statistical analysis (unpaired *t*-test) was performed using Prism (GraphPad).

Supplementary data

Supplementary data are available at *The EMBO Journal* Online (http://www.embojournal.org).

Acknowledgements

We thank Crystal Chan and Bob Lesch for purifying COPII proteins and other technical support. We thank Marcus Lee for assistance with fluorescence microscopy and Traude Beilharz for providing the GFP–Cyb5p expression construct. We thank David Fidock and David Drubin for sharing equipment. This work was supported by the NIH (GM085089 to EAM, HG01620 and GM50237 to RR, GM086530 to ELS, GM008798 to LFK, CA009503 and GM008798 to JCD and HG00193 to RJDR), the HHMI (RS) and post-doctoral fellowships from JSPS and ACS (EF).

Author contributions: LFK, SP, EF, JGD, RB, SH, ELS and EAM designed and performed the experiments. JCD, RJDR and RR contributed strains, reagents and data analysis. EAM and RS conceived the project. LFK, SP and EAM wrote the paper.

Conflict of interest

The authors declare that they have no conflict of interest.

References

Antonny B, Madden D, Hamamoto S, Orci L, Schekman R (2001) Dynamics of the COPII coat with GTP and stable analogues. *Nat Cell Biol* **3:** 531–537

Barlowe C, Orci L, Yeung T, Hosobuchi M, Hamamoto S, Salama N, Rexach MF, Ravazzola M, Amherdt M, Schekman R (1994) COPII: a membrane coat formed by Sec proteins that drive vesicle budding from the endoplasmic reticulum. *Cell* **77:** 895–907

Beilharz T, Egan B, Silver P, Hofmann K, Lithgow T (2003) Bipartite signals mediate subcellular targeting of tail-anchored membrane proteins in *Saccharomyces cerevisiae*. *J Biol Chem* **278:** 8219–8223

Bhattacharyya D, Glick BS (2007) Two mammalian Sec16 homologues have nonredundant functions in endoplasmic reticulum (ER) export and transitional ER organization. *Mol Biol Cell* **18:** 839–849

Bi X, Corpina RA, Goldberg J (2002) Structure of the Sec23/24-Sar1 pre-budding complex of the COPII vesicle coat. *Nature* **419:** 271–277

Bi X, Mancias JD, Goldberg J (2007) Insights into COPII coat nucleation from the structure of Sec23.Sar1 complexed with the active fragment of Sec31. *Dev Cell* **13:** 635–645

Bielli A, Haney CJ, Gabreski G, Watkins SC, Bannykh SI, Aridor M (2005) Regulation of Sar1 NH2 terminus by GTP binding and hydrolysis promotes membrane deformation to control COPII vesicle fission. *J Cell Biol* **171:** 919–924

Bonifacino J, Glick B (2004) The mechanisms of vesicle budding and fusion. *Cell* **116:** 153–166

Cai H, Yu S, Menon S, Cai Y, Lazarova D, Fu C, Reinisch K, Hay JC, Ferro-Novick S (2007) TRAPPI tethers COPII vesicles by binding the coat subunit Sec23. *Nature* **445:** 941–944

Dittmar JC, Reid RJ, Rothstein R (2010) ScreenMill: a freely available software suite for growth measurement, analysis and visualization of high-throughput screen data. *BMC Bioinformatics* **11:** 353

Ellenberg J, Siggia ED, Moreira JE, Smith CL, Presley JF, Worman HJ, Lippincott-Schwartz J (1997) Nuclear membrane dynamics and reassembly in living cells: targeting of an inner nuclear membrane protein in interphase and mitosis. *J Cell Biol* **138:** 1193–1206

Espenshade P, Gimeno RE, Holzmacher E, Teung P, Kaiser CA (1995) Yeast *SEC16* gene encodes a multidomain vesicle coat protein that interacts with Sec23p. *J Cell Biol* **131:** 311–324

Farhan H, Reiterer V, Korkhov VM, Schmid JA, Freissmuth M, Sitte HH (2007) Concentrative export from the endoplasmic reticulum of the gamma-aminobutyric acid transporter 1 requires binding to *SEC24D*. *J Biol Chem* **282:** 7679–7689

Futai E, Hamamoto S, Orci L, Schekman R (2004) GTP/GDP exchange by Sec12p enables COPII vesicle bud formation on synthetic liposomes. *EMBO J* **23:** 4146–4155

Gimeno RE, Espenshade P, Kaiser CA (1995) *SED4* encodes a yeast endoplasmic reticulum protein that binds Sec16p and participates in vesicle formation. *J Cell Biol* **131:** 325–338

Gimeno RE, Espenshade P, Kaiser CA (1996) COPII coat subunit interactions: Sec24p and Sec23p bind to adjacent regions of Sec16p. *Mol Biol Cell* **7:** 1815–1823

Gyuris J, Golemis E, Chertkov H, Brent R (1993) Cdi1, a human G1 and S phase protein phosphatase that associates with Cdk2. *Cell* **75:** 791–803

Hughes H, Budnik A, Schmidt K, Palmer KJ, Mantell J, Noakes C, Johnson A, Carter DA, Verkade P, Watson P, Stephens DJ (2009) Organisation of human ER-exit sites: requirements for the localisation of Sec16 to transitional ER. *J Cell Sci* **122**(Part 16)**:** 2924–2934

Iinuma T, Shiga A, Nakamoto K, O'Brien MB, Aridor M, Arimitsu N, Tagaya M, Tani K (2007) Mammalian Sec16/p250 plays a role in membrane traffic from the endoplasmic reticulum. *J Biol Chem* **282:** 17632–17639

Ivan V, de Voer G, Xanthakis D, Spoorendonk KM, Kondylis V, Rabouille C (2008) Drosophila Sec16 mediates the biogenesis of

tER sites upstream of Sar1 through an arginine-rich motif. *Mol Biol Cell* **19:** 4352–4365

Kaiser CA, Schekman R (1990) Distinct sets of SEC genes govern transport vesicle formation and fusion early in the secretory pathway. *Cell* **61:** 723–733

Kirchhausen T (2000) Three ways to make a vesicle. *Nat Rev Mol Cell Biol* **1:** 187–198

Kodera C, Yorimitsu T, Nakano A, Sato K (2011) Sed4p stimulates sar1p GTP hydrolysis and promotes limited coat disassembly. *Traffic* **12:** 591–599

Kroll ES, Hyland KM, Hieter P, Li JJ (1996) Establishing genetic interactions by a synthetic dosage lethality phenotype. *Genetics* **143:** 95–102

Kuehn MJ, Herrmann JM, Schekman R (1998) COPII-cargo interactions direct protein sorting into ER-derived transport vesicles. *Nature* **391:** 187–190

Kurihara T, Hamamoto S, Gimeno RE, Kaiser CA, Schekman R, Yoshihisa T (2000) Sec24p and Iss1p function interchangeably in transport vesicle formation from the endoplasmic reticulum in *Saccharomyces cerevisiae*. *Mol Biol Cell* **11:** 983–998

Lai CW, Aronson DE, Snapp EL (2010) BiP availability distinguishes states of homeostasis and stress in the endoplasmic reticulum of living cells. *Mol Biol Cell* **21:** 1909–1921

Lee MCS, Hamamoto S, Schekman R (2002) Ceramide biosynthesis is required for the formation of the oligomeric H+-ATPase Pma1p in the yeast endoplasmic reticulum. *J Biol Chem* **277:** 22395–22401

Lee MCS, Orci L, Hamamoto S, Futai E, Ravazzola M, Schekman R (2005) Sar1p N-terminal helix initiates membrane curvature and completes the fission of a COPII vesicle. *Cell* **122:** 605–617

Long KR, Yamamoto Y, Baker AL, Watkins SC, Coyne CB, Conway JF, Aridor M (2010) Sar1 assembly regulates membrane constriction and ER export. *J Cell Biol* **190:** 115–128

Lord C, Bhandari D, Menon S, Ghassemian M, Nycz D, Hay J, Ghosh P, Ferro-Novick S (2011) Sequential interactions with Sec23 control the direction of vesicle traffic. *Nature* **473:** 181–186

Malhotra V, Erlmann P (2011) Protein export at the ER: loading big collagens into COPII carriers. *EMBO J* **30:** 3475–3480

Mancias JD, Goldberg J (2008) Structural basis of cargo membrane protein discrimination by the human COPII coat machinery. *EMBO J* **27:** 2918–2928

Matsuoka K, Orci L, Amherdt M, Bednarek SY, Hamamoto S, Schekman R, Yeung T (1998) COPII-coated vesicle formation reconstituted with purified coat proteins and chemically defined liposomes. *Cell* **93:** 263–275

Miller E, Antonny B, Hamamoto S, Schekman R (2002) Cargo selection into COPII vesicles is driven by the Sec24p subunit. *EMBO J* **21:** 6105–6113

Miller EA, Barlowe C (2010) Regulation of coat assembly—sorting things out at the ER. *Curr Opin Cell Biol* **22:** 447–453

Miller EA, Beilharz TH, Malkus PN, Lee MCS, Hamamoto S, Orci L, Schekman R (2003) Multiple cargo binding sites on the COPII subunit Sec24p ensure capture of diverse membrane proteins into transport vesicles. *Cell* **114:** 497–509

Miller EA, Liu Y, Barlowe C, Schekman R (2005) ER-Golgi transport defects are associated with mutations in the Sed5p-binding domain of the COPII coat subunit, Sec24p. *Mol Biol Cell* **16:** 3719–3726

Mossessova E, Bickford LC, Goldberg J (2003) SNARE selectivity of the COPII coat. *Cell* **114:** 483–495

Mumberg D, Muller R, Funk M (1994) Regulatable promoters of *Saccharomyces cerevisiae*: comparison of transcriptional activity and their use for heterologous expression. *Nucleic Acids Res* **22:** 5767–5768

Pagant S, Kung L, Dorrington M, Lee MCS, Miller EA (2007) Inhibiting endoplasmic reticulum (ER)-associated degradation of misfolded Yor1p does not permit ER export despite the presence of a diacidic sorting signal. *Mol Biol Cell* **18:** 3398–3413

Parlati F, McNew J, Fukuda R, Miller R, Sollner T, Rothman J (2000) Topological restriction of SNARE-dependent membrane fusion. *Nature* **407:** 194–198

Pucadyil TJ, Schmid SL (2009) Conserved functions of membrane active GTPases in coated vesicle formation. *Science* **325:** 1217–1220

Reid RJ, Gonzalez-Barrera S, Sunjevaric I, Alvaro D, Ciccone S, Wagner M, Rothstein R (2011) Selective ploidy ablation, a high-throughput plasmid transfer protocol, identifies new genes affecting topoisomerase I-induced DNA damage. *Genome Res* **21:** 477–486

Rexach MF, Schekman RW (1991) Distinct biochemical requirements for the budding, targeting, and fusion of ER-derived transport vesicles. *J Cell Biol* **114:** 219–229

Saito Y, Yamanushi T, Oka T, Nakano A (1999) Identification of *SEC12*, *SED4*, truncated *SEC16*, and *EKS1/HRD3* as multicopy suppressors of ts mutants of Sar1 GTPase. *J Biochem* **125:** 130–137

Saito-Nakano Y, Nakano A (2000) Sed4p functions as a positive regulator of Sar1p probably through inhibition of the GTPase activation by Sec23p. *Genes Cells* **5:** 1039–1048

Sato K, Nakano A (2005) Dissection of COPII subunit-cargo assembly and disassembly kinetics during Sar1p-GTP hydrolysis. *Nat Struct Mol Biol* **12:** 167–174

Schuldiner M, Collins S, Thompson N, Denic V, Bhamidipati A, Punna T, Ihmels J, Andrews B, Boone C, Greenblatt J, Weissman J, Krogan N (2005) Exploration of the function and organization of the yeast early secretory pathway through an epistatic miniarray profile. *Cell* **123:** 507–519

Settles EI, Loftus AF, McKeown AN, Parthasarathy R (2010) The vesicle trafficking protein Sar1 lowers lipid membrane rigidity. *Biophys J* **99:** 1539–1545

Shaywitz DA, Espenshade PJ, Gimeno RE, Kaiser CA (1997) COPII subunit interactions in the assembly of the vesicle coat. *J Biol Chem* **272:** 25413–25416

Sikorski R, Hieter P (1989) A system of shuttle vectors and yeast host strains designed for efficient manipulation of DNA in *Saccharomyces cerevisiae*. *Genetics* **122:** 19–27

Snapp EL, Hegde RS, Francolini M, Lombardo F, Colombo S, Pedrazzini E, Borgese N, Lippincott-Schwartz J (2003) Formation of stacked ER cisternae by low affinity protein interactions. *J Cell Biol* **163:** 257–269

Springer S, Schekman R (1998) Nucleation of COPII vesicular coat complex by endoplasmic reticulum to Golgi vesicle SNAREs. *Science* **281:** 698–700

Springer S, Spang A, Schekman R (1999) A primer on vesicle budding. *Cell* **97:** 145–148

Stagg SM, LaPointe P, Balch WE (2007) Structural design of cage and coat scaffolds that direct membrane traffic. *Curr Opin Struct Biol* **17:** 221–228

Supek F, Madden DT, Hamamoto S, Orci L, Schekman R (2002) Sec16p potentiates the action of COPII proteins to bud transport vesicles. *J Cell Biol* **158:** 1029–1038

Tabata K, Sato K, Ide T, Nishizaka T, Nakano A, Noji H (2009) Visualization of cargo concentration by COPII minimal machinery in a planar lipid membrane. *EMBO J* **28:** 3279–3289

Watson P, Townley AK, Koka P, Palmer KJ, Stephens DJ (2006) Sec16 defines endoplasmic reticulum exit sites and is required for secretory cargo export in mammalian cells. *Traffic* **7:** 1678–1687

Whittle JRR, Schwartz TU (2010) Structure of the Sec13-Sec16 edge element, a template for assembly of the COPII vesicle coat. *J Cell Biol* **190:** 347–361

Witte K, Schuh AL, Hegermann J, Sarkeshik A, Mayers JR, Schwarze K, Yates JR, Eimer S, Audhya A (2011) Mechanisms by which TFG functions in protein secretion and oncogenesis. *Nat Cell Biol* **13:** 550–558

Yoshihisa T, Barlowe C, Schekman R (1993) Requirement for a GTPase-activating protein in vesicle budding from the endoplasmic reticulum. *Science* **259:** 1466–1468

Zacharogianni M, Kondylis V, Tang Y, Farhan H, Xanthakis D, Fuchs F, Boutros M, Rabouille C (2011) ERK7 is a negative regulator of protein secretion in response to amino-acid starvation by modulating Sec16 membrane association. *EMBO J* **30:** 3684–3700